LIGO Laboratory / LIGO Scientific Collaboration

LIGO- T2200011-v2 *LIGO* 28 Jan 2022

Optical Absorption Limits on Hydrocarbon Partial Pressure

Dennis Coyne

Distribution of this document:
LIGO Scientific Collaboration

This is an internal working note
of the LIGO Laboratory.

California Institute of Technology
LIGO Project

Massachusetts Institute of Technology
LIGO Project

LIGO Hanford Observatory

LIGO Livingston Observatory

http://www.ligo.caltech.edu/

Table of Contents

List of Figures

List of Tables

1 Introduction

High molecular weight hydrocarbons (AMUs > 100) can be deleterious to the LIGO interferometer by either

a) causing phase noise due to scattering if their density is high enough in the 4 km long arms, or by
b) deposition onto sensitive optics resulting in increased optical loss by absorption and/or by scattering.

The required[1] (and goal[2]) hydrocarbon partial pressures were established for the Advanced LIGO (aLIGO) project as indicated in Table 1.

Table 1 Hydrocarbon Partial Pressure Limits in the 4 km long Beam Tubes, from Residual Gas Scattering

Gas Species	aLIGO Requirement (torr)	Goal (torr)
AMU 100 Hydrocarbon	2×10^{-12}	7×10^{-13}
AMU 300 Hydrocarbon	2.2×10^{-13}	5×10^{-14}
AMU 500 Hydrocarbon	9×10^{-14}	1×10^{-14}

As a practical matter we have only been able to achieve a HC partial pressure of ~2 to 3 x 10^{-12} Torr and (fortunately) we've found this quality of vacuum to be sufficient … so far. While this is close to the aLIGO required partial pressures given in Table 1, we will soon operate the LIGO detector in the O4 Science run with a number of improvements including an increase in Fabry-Perot arm cavity power.

Moreover, as noted in the Advanced LIGO (aLIGO) Acceptance Document[3], the theoretical model connecting hydrocarbon (HC) partial pressure to an optical absorption rate increase due to a putative molecular film deposition, has not been experimentally confirmed. The limit on the partial pressure of high mass hydrocarbon (HC) partial pressure was speculated to be < ~2 x 10^{-15} Torr in order to limit the accumulation to < 0.1 monolayer per year[4] (albeit using conservative parameters).

This memo attempts to:

1) provide some possible explanations for the apparent discrepancy between the speculated partial pressure limit for deposition onto sensitive optics and performance to date,
2) establish a modeling framework to use for establishing a revised HC partial pressure limit (for LIGO vacuum Review Board (VRB) approval), and
3) make recommendations for further study/work.

2 Contamination induced optical loss experience

LIGO experience with hydrocarbon partial pressure and optical loss is summarized in the following subsections. Hydrocarbons with high Atomic Mass Units (AMU) crack into lower AMU components when measured by a mass spectrometer. AMUs 41, 43, 53, 55 and 57 were found to be indicative of all high molecular weight hydrocarbons[5] and so we sum the partial pressures of these as "flag" AMUs to determine the hydrocarbon partial pressure[6]. (When evaluating the hydrocarbon cleanliness of a

component or vacuum volume, the mass spectrum should also not have any AMU peaks greater than 44 which are significantly above the instrument noise floor.)

2.1 aLIGO Observatories

2.1.1 HC partial pressure

The HC partial pressures in the LIGO vacuum volumes[7] which house the interferometer components (i.e. the vacuum system except for the 4 km long beam tubes) are about 12 pTorr without the benefit of pumping from the cryopumps and the beam tubes. When all large gate valves are open the HC partial pressure[8] is 2 to 3 pTorr; see Figure 1. This apparent HC partial pressure is near the noise floor of the RGA instrument; An accumulation measurement would be needed to make a more accurate measurement. Whether this represents the cracked components of high AMU molecules, or simply light hydrocarbons (e.g. solvents) is not currently known.

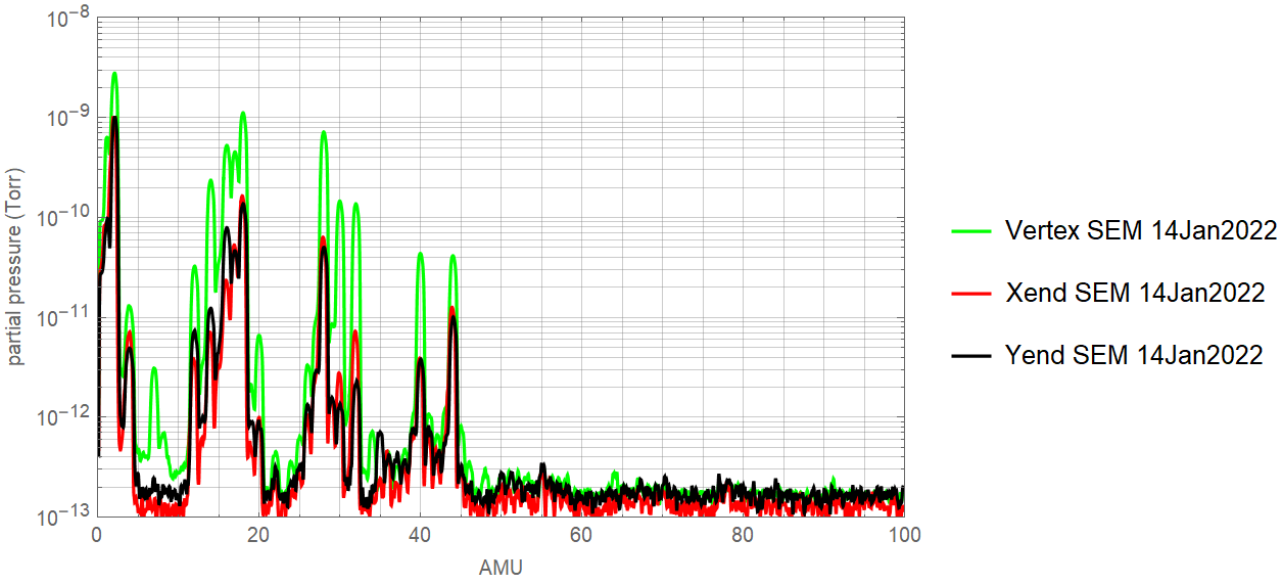

Figure 1 Mass spectrum for the vacuum volumes with interferometer components @LLO

2.1.2 Test Mass Optics

Fits to in situ HWS measurements imply low uniform absorption values for the TMs, see e.g. LLO elog#47493 (23-Aug-2019). These fits are likely not accurate due to the presence of point absorbers. Nonetheless this data does not suggest significant increase in the uniform coating absorption despite being in the vacuum system for many years with HC partial pressures in the pTorr (10^{-12} Torr) range.

2.1.3 Input Mode Cleaner (IMC)

In the period from Jan 2013 through April 2014 we were concerned about a possible increase (secular trend) in optical absorption in the IMC at LLO. Although there are some ambiguities and uncertainties in the measurements, the absorption appeared to increase from ~1 ppm per mirror to ~5 ppm per mirror. At first it seemed that the increased absorption might be the result of venting the vacuum system (see LLO elog #9095). However, the variation in IMC absorption was eventually found to be related to beam spot position (see e.g. LLO elog #11884 and #12033). Particulate

contamination, coating point defects and/or "clumpy" deposition of sub-monolayer molecular contamination might explain these variations.

2.2 LIGO 40m Interferometer

Molecular contamination of the vacuum system of the 40m experimental interferometer at Caltech during the argon-ion laser era caused significant problems[9]. The contamination resulted in anomalous loss of > 100 ppm per test mass optic. The cause was thought to be primarily due to unbound fluorine emission from the fluoroelastomer springs used in the isolation system. The fluorine when combined with water upon vacuum system vents would create hydrofluoric acid which could etch/alter the optical coatings. Another possible explanation is laser induced cracking of deposition products on the mirrors, which might lead in turn to increased absorption. While cracking can occur at the photon energy levels for the argon-ion laser (514 nm), it is not likely an issue for the Nd:YAG wavelength (1064 nm); see section 6. The hydrocarbon partial pressure (sum of AMUs 41, 43, 53, 55 and 57) was ~7 x 10^{-11} Torr – about 20 times higher HC partial pressure than the aLIGO observatory vacuum systems.

2.3 LIGO Ring-down cavities for material qualification testing

2.3.1 1064 nm wavelength

In-vacuum materials qualification process[10,11] for LIGO requires testing in an optical ring-down cavity[12] in addition to a Residual Gas Assay (RGA) with a mass spectrometer. The optical loss measurement system is based on a resonant Fabry-Perot cavity at 1064 nm in vacuum. Total optical loss is derived from the ring-down response of the cavity. Absorption loss is calculated from the shift in the beat frequency of two resonant TEM modes; The shift is a result of a change in curvature due to surface absorption. The basic idea is to replicate the optical conditions of the LIGO core optics (irradiance level, vacuum level) while exposed to the outgassing from a material under consideration. The amount of material in the test as compared to the proposed application and the hydrocarbon pumping rate of the test as compared to the LIGO Observatory vacuum system are used to scale the results. We attempt to emulate the operational conditions for the core optics.

As indicated in section 4, the overall limit on contamination induced optical loss is < 0.5 ppm/yr absorption and < 4 ppm/yr scatter from all contamination sources. For ring-down cavity test qualification we assume that ~20 sources could contribute, so we set the acceptance criteria to < 0.02 ppm/yr maximum absorption and < 0.2 ppm/yr maximum scatter from a single source, at the 2-sigma level. An example of the test results is shown in Figure 2. Typically we test for a duration of ~2 to 3 months in order to reduce the uncertainty in the least squares fit of absorption and total loss over time.

This test is a "null test"; We don't measure loss rate but instead set a limit on the maximum possible loss rate for the conditions of the test. Quite often the loss appears to decrease with time. This might be due to adsorbed species from the air (water, hydrocarbons) being pumped and thermally excited off of the substrate in vacuum. These initial adsorbed layers might be masking the substrate from any molecular outgassing from the test material. Alternatively the secular trends in absorption and total loss (scatter) may be a result of a slow pointing drift coupled with non-uniformity of the cavity mirror coatings.

As explained in section 9, High Reflectance (HR) coatings designed with near zero electric field strength at their surface are inherently insensitive to the effects of contamination. By using mirrors in the ring-down cavities which have near-zero electric field strength at their surface we have faithfully emulated the LIGO interferometer test mass optics, but we have made the test system insensitive to measurement of the effects of adsorbed outgassing contaminants. This is likely why attempts to actually measure the increased optical loss due to "dirty" materials (e.g. mineral oil, unbaked Viton) have failed. In fact none of the optical cavity exposure tests to date[13] show an increase in optical absorption even at ~10 times the HC partial pressure in our observatory chambers.

The optical ring-down cavities were originally designed and put into operation for Initial LIGO (iLIGO) in 1999. The peak mirror intensity at that time was designed to match the peak irradiance anticipated for iLIGO, 150 kW/cm^2 (as stated in Reference 12). The current set of three ring-down cavities at Caltech operate with a peak irradiance of 690 kW/cm^2. The ultimate peak irradiances for the aLIGO and A+ LIGO mirrors are somewhat higher, as shown in Table 2. As a consequence the photon flux in the ring-down cavity tests are less than we ultimately plan to operate with the LIGO Observatories. Although unlikely it is possible that Multiple Photon Dissociation (MPD; see section 6) could occur in operation but not be caught in our ring-down cavity tests unless we increase the irradiance.

2.3.2 514 nm wavelength

Prior to the decision to use Nd:YAG lasers at 1064 nm wavelength an optical test facility was built at Caltech using an argon ion laser at 514 nm wavelength. A catastrophic increase in the optical loss of the resonator was observed at one point in its operation[14]. Rutherford Backscattering Spectrometry (RBS) and Scanning Electron Microscopy (SEM) were used to examine the surface damage. The conclusion was that residue from an Alcanox cleaning solution was responsible for the carbon contamination. Since the optical loss increased with exposure time (on the order of 2 days) with ~5 kW/cm^2 fluence the carbon growth was likely due to photodissociation.

Table 2 Peak Irradiances for aLIGO and A+ LIGO

Optic	Peak Irradiance (kW/cm^2)
IMC	167
PRM	34
PR2, PR3, BS HR CP & ITM AR	~6
ITM HR	850
ETM HR	621

Figure 2 Optical ring-down cavity example result for an epoxy-coated aluminum foil

Non-reflective Black Foil (All Foils; ThorLabs BKF12)

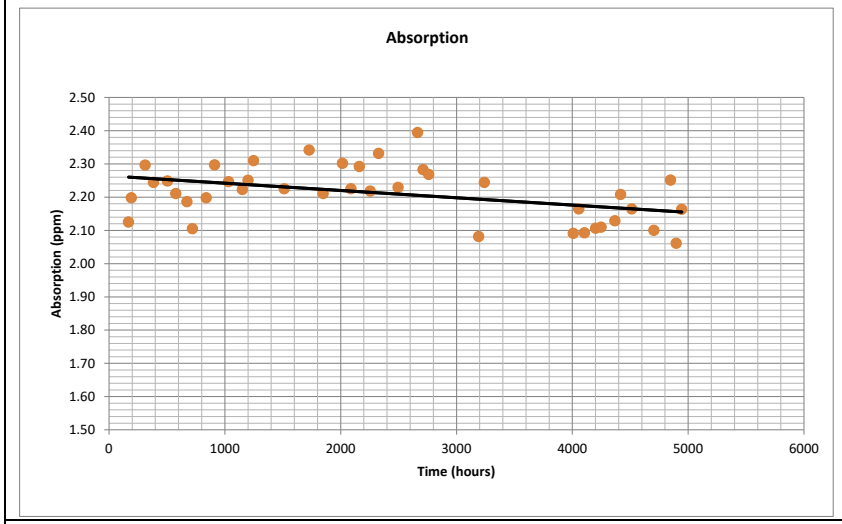

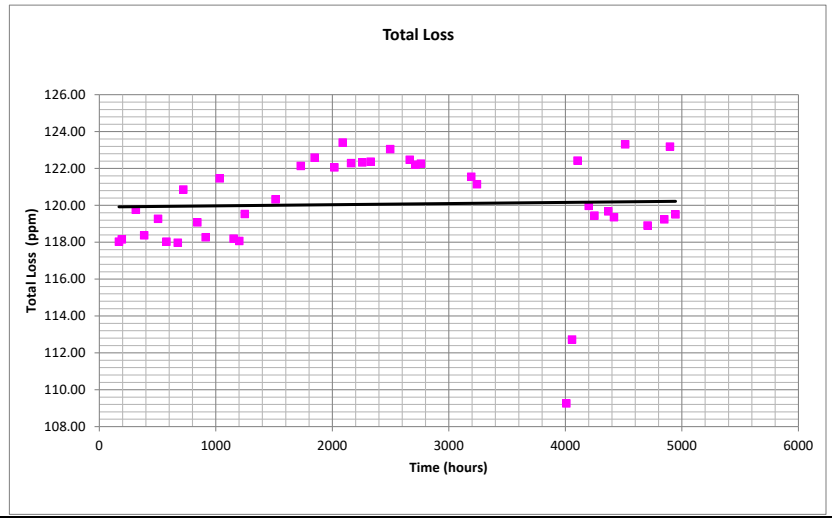

LIGO E-Document Number:			**E1900232**				
Sample Test:							
	Material under test:			**Non-Reflective Black Foil (All Foils; ThorLabs BKF12)**			
	units			92903	cm^2		including both sides
	absorption	-0.19237	±	0.06614437	ppm/yr	1 sigma	
	scatter	0.552045	±	2.51541496	ppm/yr	1 sigma	
	max. normalized absorption			0.00E+00	ppm/yr/unit	2 sigma	
	max. normalized scatter			6.01E-05	ppm/yr/unit	2 sigma	
	test turbopump speed (liter/s)			24.391574	torr/liter/sec		
Scaled to LIGO:							
	LIGO Vacuum Volume			**Vertex**	**LHO Diagonal**	**End**	**Comments**
	Quantity (units)			55500	0	55500	cm^2 including both coated sides; based on surrounding the Transmission Monito Suspension in the end stationand assuming a comparable amount used in the vertex
	LIGO ion pumping speed (liter/s)			6800	6800	1700	see E0900398 or PSI V049-1-078 for pump rates
	pumping speed ratio (test/LIGO)			0.0036	0.0036	0.0143	does not include cryo-pump and effective pumping from the Beam Tube
	max. absorption (ppm/yr)			0.000	0.000	0.000	* Limit is < 0.02 ppm/yr for a single source
	max. scatter (ppm/yr)			0.012	0.000	0.048	* Limit is < 0.2 ppm/yr for a single source

2.4 Commercial EUV systems

Commercial EUV systems use unbaked vacuum systems because the Mo/Si multilayer optical coatings are sensitive to elevated temperatures (which cause interdiffusion). Much like LIGO, the inability to bake the vacuum system creates an environment with residual water vapor and hydrocarbons (outgassed from materials used to construct the lithography equipment such as cables, stages, etc.). This residual gas environment presents a threat to the EUV optics, just as it does for LIGO. However, the EUV-induced decomposition of the adsorbed species is a more serious threat (due to the smaller wavelengths, higher energy) than it is for LIGO (see section 6). Note that the typical RGA scan of the Sandia National Labs' ETS main vacuum chamber (Figure 3) has ~5 times higher hydrocarbon partial pressure than the LIGO Observatory vacuum volumes (Figure 1). The ETS is an engineering test system developed to demonstrate the overall feasibility of EUV Lithography (EUVL) technology.

Figure 3 Typical RGA scan of the Sandia National Labs ETS main chamber[15]

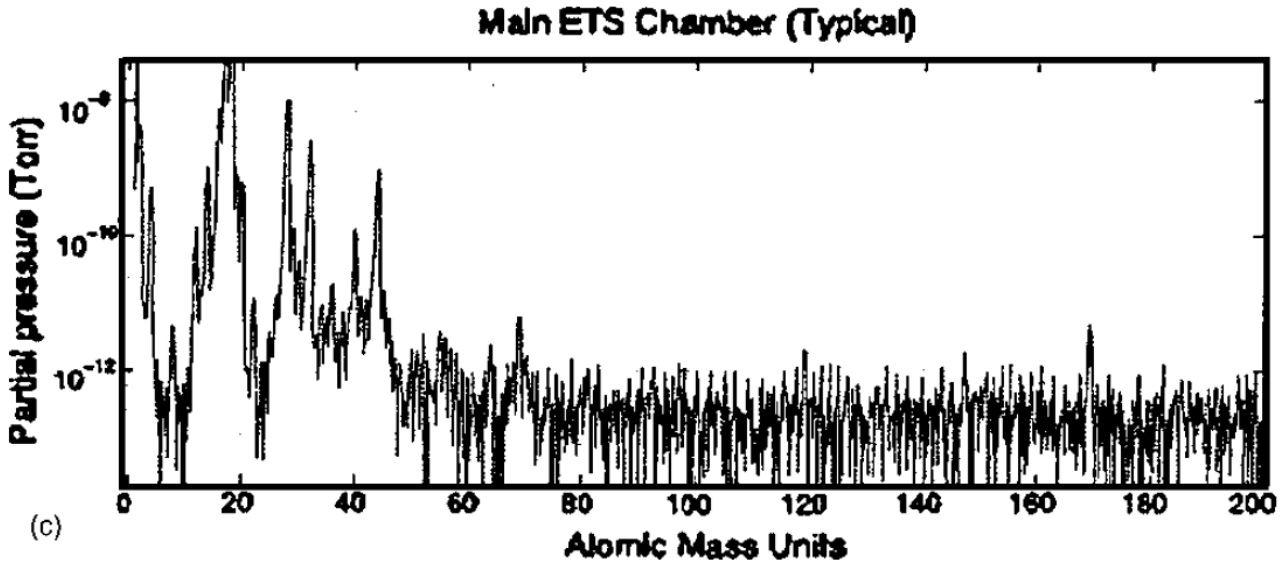

3 Hydrocarbon partial pressure limit set by scattered light phase noise

The hydrocarbon partial pressures limits derived for the Advanced LIGO (aLIGO) project in Reference [1] and listed in section 1 of this memo still apply. However, note that the allowable partial pressures in the vertex and end stations, due solely to scattered light phase noise considerations in the 4km arm cavities, can be higher due to the attenuation through the cryopumps and the fact that the beam tube surface acts as a near infinite capacity pump; *This is beyond the scope of this memo.*

4 Optical loss limits due to accumulated hydrocarbon contamination

Allowable limits on residual gas due to optical loss (scattering and absorption) as a result of adsorbed/condensed species on the optics was not addressed in Reference [1], but are addressed in the balance of this memo.

4.1 Test Mass HR coatings

The LIGO Core Optic Component (COC) design limit for optical loss due to contamination on Surface 1 (the HR surface) is:

- < 0.5 ppm/yr absorption, and
- < 4 ppm/yr scatter

from all sources, per Table 5 and section 4.2.5 of the Advanced LIGO COC Design Requirements Document (T000127-v4).

4.2 Test Mass AR coatings

The COC Design Requirements Document does not specify limits to cumulative contamination absorption or scattering for Surface 2 (AR). The AR absorption should be small relative to the substrate bulk absorption, which is < 40 ppm. So, let's take < 4 ppm/yr for AR absorption due to surface contamination.

4.3 Beamsplitter (BS)

The Beamsplitter (BS) coating specification, LIGO-E0900073, requires both surfaces to have absorption < 1 ppm. However, waiver LIGO-E1500055 establishes that the BS AR surface (surface 2) can have up to 2 ppm absorption and be acceptable.

4.4 Compensation Plate (CP)

The Compensation Plate (CP) coating specification, , requires that both AR surfaces have absorption < 1 ppm. However, LIGO-T1400071 accepts CP-09 with 2.7 ppm on surface 2.

4.5 Input Optics (IO)

The Input Optics Design Requirements Document (T0900386) does not specify limits to cumulative contamination absorption or scattering. However document T060077, points out that mode matching using the DKDP passive compensation element can only compensate for ~1 ppm surface absorption. With the inherent absorption of a pristine coating being ~0.5 ppm, this only permits ~0.5 ppm due to surface contamination. With the same cleaning maintenance period as for COC this implies a absorption limit due to the cumulative contamination of 0.5 ppm/yr on HR surfaces.

5 Optical scatter from contaminant film

Previous studies[16,17,18,19] have demonstrated the contaminants such as pump oil are deposited in droplet form ("clumps") on mirror surfaces which result in substantial specular reflectance loss and an increase in BRDF. Some of these studies[17,18] indicate that the reflectance losses are temporary and gradually recover after the contamination source is diminished or removed, as long as the contaminant film is not 'cracked' or photopolymerized. As shown in section 10, for low partial pressures the residual molecular film thickness is less than one monolayer. I suspect that as the adsorbed contaminant layer approaches 1 monolayer the optical scattering loss becomes negligible. *However further literature review and/or experimentation is required to establish a scattering loss model as a function of HC partial pressure over fused silica.*

6 Cracking

Carbon contamination growth occurs on optics exposed to high energy irradiation such as synchrotron radiation[20] and extreme ultraviolet (EUV) radiation[21,22,23,24] and solar UV exposure on orbit. The carbon growth is the result of breaking ('cracking') the hydrocarbon bonds of molecular species deposited/adsorbed onto optical surfaces. The mean C-H bond enthalpy is 412 kJ/mol and the mean C-C bond enthalpy is 348 kJ/mol. A single photon of wavelength 289.5 nm or shorter (342.7 nm or shorter) has sufficient energy to break a typical C-H bond (C-C bond). Single infrared (or near infrared, NIR) photons are not energetic enough for direct photodissociation of molecules.

However, a molecule could gain sufficient internal energy to dissociate after absorption of multiple infrared photons. Multiple Photon Dissociation (MPD) can be achieved by application of high power lasers, and by long interaction times of the molecule with the radiation field without the possibility for rapid cooling, e.g. by collisions. In general, the energy requirement is such that the absorbed energy must correspond to the quantized energy levels between excited states. The minimum energy quantization between excited states is typically about ~1 eV (election volt) or 2 x 10^{-19} J, which corresponds to a wavelength of about 1 μm. At least 4 photons at 1064 nm must be absorbed by a HC molecule before energy is lost through other mechanisms in order to break a C-C bond. Given that the photon absorption cross-sections for NIR are ~10 times smaller than for EUV, this is quite unlikely, even for very high photon flux. In fact this is one of the reasons that Nd:YAG was chosen as the LIGO laser source rather than argon-ion laser (514 nm).

Experimental evidence[22] indicates that EUV molecular dissociation does not occur in the gas phase above the optic surface (at least for partial pressures < 10^{-5} Torr). Only adsorbed molecules on the surface of the optic can dissociate and contribute to a carbonaceous film.

The ring-down cavity tests (see section 2.3) are designed to subject the test optics exposed to polymer/hydrocarbon materials at the highest irradiance in the Advanced LIGO system to see if MPD can occur for any of the contaminant species that we might have in our vacuum system. No obvious MPD has occurred in the testing to date. However, note that the ultimate irradiance levels for aLIGO/A+ are somewhat higher than developed in the ring-down cavities; see section 2.3.

7 Optical absorption as a function of contaminant species and film thickness

7.1 General guidance

A simple approximation to the amount of light absorbed by a contaminant film of the surface of a transmitting medium is given by Beer's Law (also referred to as the Lambert-Bouguer transmittance law):

$$I = I_0 e^{-\alpha t}$$

Where I is the transmitted intensity, I0 is the incident intensity, α is the absorption coefficient of the contaminant (1/Å) and t is the contaminant layer thickness (Å).

A study by Welsh and Jelinsky[25] reported measurements of the reflectance change due to deposition of ten polymer materials which are commonly used in space instruments in the spectrum from UV to near IR (120 nm to 1100 nm wavelength) as a function of contaminant layer thickness (from 50 to 500 Angstroms). As typical in these studies, the deposition thickness was measured with a quartz

crystal microbalance. Although the deposition surface of the quartz crystal was not described, it was likely gold plated[26]. The witness mirror is described as "super-smooth, high reflectance (R > 98%) gold coated". A thin protective overcoat of SiO2, although not uncommon for metal coated mirrors, was not mentioned in this study, The results were summarized in terms of the absorption coefficient, α, of Beer's Law as a function of wavelength. At 1 micron wavelength, α ranges from 3 - 12 x 10^{-4} (1/Å). This implies that 1 ppm of absorption would result from a 0.0008 to 0.003 Å thick contaminant layer. However the authors noted:

1) Their absorption coefficients at visible wavelengths are in significant disagreement with previously published values (up to 50 times greater), and
2) To accurately determine the absorption coefficient the complex refractive indices of the contaminant and thin film reflectance theory is really needed.

The optical absorption of one the materials in the Welsh and Jelinsky study, an epoxy adhesive (3M Scotch-Weld EC2216) was also measured in the same spectral range in a study by Shimazaki et. al.[27] The Shimazaki et. al. study used an uncoated quartz (SiO2) substrate/optic as well as quartz crystal microbalances to measure the deposition thickness. This study found no reduction in transmittance (to a resolution of ~0.5%) at 1 micron wavelength for epoxy contaminant thickness up to 30 nm. In contrast, using the absorption coefficient from the Welsh and Jelinsky study for this same epoxy (9.9 to 11.6 x 10^{-4} 1/Å) would imply a 26% absorption. Shimazaki et. al. used their measurements to infer the complex refractive index of the epoxy as a function of wavelength.

Another significant result from the Shimazaki et. al. study was that optical transmittance decrease that they measured due to epoxy outgassing deposition at -80 C, was completely reversed (to a resolution of ~0.5%) above 0 C. The epoxy out-gassed deposition thickness (as measured by the quartz crystal microbalance) was still 3 nm thick at 25 C (after depositing 30 nm at -80 C). From this we can infer that:

1) The saturation thickness of the epoxy at 25C is ≤ 3 nm (with a dwell time of ~30 minutes and assuming no temperature hysteresis), and
2) A 3 nm thickness of the out-gassed components of this particular epoxy causes a transmittance loss of < ~ 0.5%.

The most significant difference between the Welsh and Jelinsky and the Shimazaki et. al. studies is the use of a gold coated reflective optic in the former and a quartz (fused silica) transmissive optic in the later. Additionally the vacuum pressure was quite likely significantly lower[28] in the Shimazaki et. al. study.

7.2 Contamination sensitivity of multilayer dielectric coatings

General guidance regarding molecular contamination dismiss interference and scattering for infrared instruments since $\lambda/4$ would be quite thick.[29,30] While this is true, the interaction of the surface contaminant film with the electric field created by the presence of a multilayer dielectric coating can be significant for contamination layers much thinner than $\lambda/4$. In addition, the presence of even a thin contaminant layer can alter the coating admittance, Y_0. As a consequence, in order to calculate the effect of thin contaminant films on the reflectivity, transmissivity and absorption of optics with multilayer dielectric coatings, one must incorporate the complex refraction index of the contaminant.

The absorbed energy areal density in a thin film is given by[31]:

$$I_{absorbed} = \frac{2\pi nkd}{\lambda} Y_0 E^2$$

The absorption due to a contaminant layer then depends upon the product of the index of refraction, n, the extinction coefficient, k, the thickness, d, and the electric field amplitude at the surface, E, squared.

Since we have (in some cases; see section 9) specified the maximum electric field strength at the surface, one might think we can readily calculate the contaminant film absorption if we know the n and k values for wavelength λ. However, the electric field gradient can be extremely large (especially for a HR design) and the presence of even a thin contaminant layer alters the admittance of the coating significantly. It is best to use an optical coating design/analysis program to calculate the effect of a contaminant layer, as is done in section 9 for LIGO core optics.

8 Complex refraction indices of HC contaminants

Two separate, comprehensive measurement studies of the wavelength variation (visible through IR) of the complex refraction parameters of the following seven polymer materials were conducted with the same methodology and authors[32,33]:

- polydimethylsiloxane (PDMS),
- polymethyl methacrylate (PMMA),
- polycarbonate (PC),
- polystyrene (PS),
- polyethylene terephthalate (PET),
- polyvinyl chloride (PVC), and
- polyetherimide (PEI)

These measurements were made directly on the material samples, not on the deposition of out-gassed material from these samples. The authors argue that highly transparent materials with weak absorption cannot be accurately measured with the common reflection-transmission (RT) method, the Kramers-Kronig transform method or spectroscopic ellipsometry (SE). Their method is spectroscopic ellipsometry (SE) coupled with the Ray Tracing Method (RTM) and the Double-Optical Pathlength Transmission Method (DOPTM).

Their results are plotted in Figure 4. In the region of interest for the LIGO interferometer (532 nm to 1064 nm) there is very little variation or structure. The extinction coefficient (k) does show some variation from ~880 nm to ~1020 nm, but the values are small ($< 10^{-5}$).

The significant structure in the wavelength dependence from 5 to 15 microns (667 to 2,000 1/cm) is associated with deformation (bending, stretching) of chemical bonds (C-C, C-H, etc.) in the molecules. This structure in the wavelength dependence in IR is what we use with FTIR testing to identify the contaminants on our surfaces.

The values from this data set very near the LIGO laser wavelength (measured at 1060 nm vs 1064 nm), are given in Table 3. The maximum k *n value for this set of seven polymers is 3×10^{-6}.

The complex refraction parameters of hydrocarbons from a number of other studies are also included in Table 3. Some of these measurements are for the material directly and not the outgassed products. The maximum n * k product at 1064 nm is:

- Set A: 0.064, pessimistic; considering all the data in Table 3 including Conoco HD2 grease, Methyl Siloxane mold release agent (silicone) and palm oil
- Set B: 0.0035, conservative; if we accept spectroscopic ellipsometry (SE) data for low loss measurements
- Set C: 3×10^{-6}, possible; if we accept the argument in Reference 33 that the extinction values from other methods may not be very accurate since the absorption near 1 micron is rather weak.

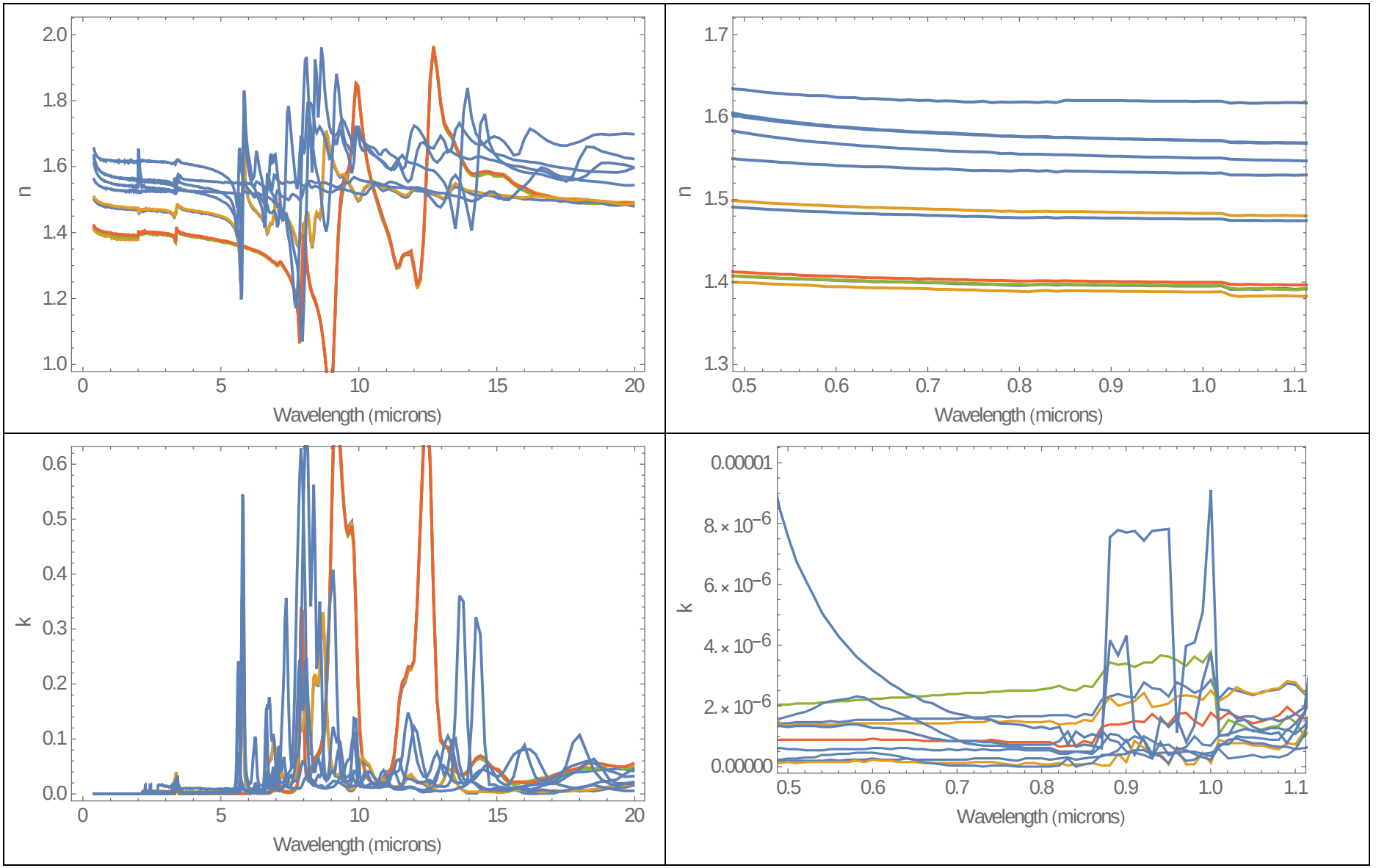
n
Wavelength (microns)
n
Wavelength (microns)
k
Wavelength (microns)
k
Wavelength (microns)

Figure 4 Refraction indices (n) and extinction coefficients (k) from 0.4 to 20 microns

Table 3 Complex refractive indices for various polymers at 1064 nm wavelength

[reference]Material	λ (μm)	n	k (x 10^{-6})	n * k (x 10^{-6})	Notes
[37]AS4/J2 thermoplastic composite outgassing products on Germanium	2.5	1.2	< 0.001	< 0.0012	
[37]Chemglaze Z306	2.5	1.3	< 0.001	< 0.0013	
[34]Conoco HD2 grease	~1.064	3.2	.02	0.064	SE
[35]DC-704 silicone oil	.3 to 1	1.6	~5 x 10^{-5}	~ 0.00008	
[36]bis-diethylhexylphatate (DEHP) film on fused silica	~0.7	1.7	0.002	0.0034	Photochemical deposition; k falling as λ increases
[27]EC2216 3M Scotch-Weld adhesive epoxy outgassing products on quartz	1.064	1.41	0.0025	0.0035	transmission spectrometer
[34]Methyl Siloxane mold release agent (silicone)	~1.064	1.7	.02	0.034	SE
[37]Mylar film outgassing products on Germanium	2.5	1.25	< 0.001	< 0.0012	
[38]palm oil and palm oil biodiesel	2.44	1.39	5 x 10^{-3}	0.0070	Combined SE-transmission
[33]polydimethylsiloxane (PDMS) outgassing products on quartz	1.06	1.39	1.92 x 10^{-6}	2.67 x 10^{-6}	SE, RTM, DOPTM
[33]polymethyl methacrylate (PMMA) outgassing products on quartz	1.06	1.48	0.965 x 10^{-6}	1.42 x 10^{-6}	SE, RTM, DOPTM
[33]polycarbonate (PC) outgassing products on quartz	1.06	1.57	0.318 x 10^{-6}	0.499 x 10^{-6}	SE, RTM, DOPTM

[33]polystyrene (PS) outgassing products on quartz	1.06	1.57	0.936×10^{-6}	1.47×10^{-6}	SE, RTM, DOPTM
[33]polyethylene terephthalate (PET) outgassing products on quartz	1.06	1.55	1.15×10^{-6}	1.78×10^{-6}	SE, RTM, DOPTM
[33]polyvinyl chloride (PVC) outgassing products on quartz	1.06	1.53	0.777×10^{-6}	1.19×10^{-6}	SE, RTM, DOPTM
[33]polyetherimide (PEI) outgassing products on quartz	1.06	1.62	1.56×10^{-6}	2.52×10^{-6}	SE, RTM, DOPTM
[39]Polyurethane resPUR-OT-T24000	0.9	1.48	1×10^{-5}	1.48×10^{-5}	
[40]diglycidyl either of bisphenol A, (DGEBA) (kimapoxy 150), with cycloaliphatic polyamine as curing agent	0.5	~1.1	$\sim 4 \times 10^{-4}$	$\sim 4 \times 10^{-4}$	

9 LIGO Optic sensitivity to contamination

The optical coatings for the Advanced LIGO (aLIGO) Core Optics Components (COC) were provided by Laboratoire Matériaux Avancés (LMA). All of the LMA coating designs are proprietary; The data given in the following subsections is not proprietary. However the coating design references given below have restricted access in the LIGO Document Control Center (DCC).

9.1 ETM HR

9.1.1 Specification

The High Reflectance (HR) coating specification for the End Test Mass (ETM) is given in LIGO-E0900068 as follows:

- Transmittance, T = 5 ppm +/- 1 ppm @1064 nm wavelength
- Absorptance, A < 0.5 ppm
- Surface electric field @1064 nm, E < 0.01 V/m; The vendor must demonstrate meeting this surface electric field limit through calculation using this equation[41]:

  E [V/m] = (27.46) (T P / Re (Y))1/2

  with

  T = 6E-6 (6 ppm) surface transmittance,

  Y = the admittance in free space units, and

  P = 1 W/m2 as the incident power density.

In SI units the admittance of free space is

$$Y_0 = \sqrt{\varepsilon_0/\mu_0} = 0.0026544\ Siemens \text{ and } \sqrt{2/Y_0} = 27.45$$

where

ε_0 = permittivity of a vacuum

μ_0 = permeability of a vacuum

9.1.2 Coating design

LMA's proprietary ETM HR coating design is given in LIGO-C1000251. The transmission, absorption and electric field distribution for the ETM HR coating, calculated with a modified version of the Matlab script jreftrans_rt.m[42], agrees reasonably well with the specification:

- T = 3.6 ppm
- A = 0.6 ppm
- E = 0.0142 V/m

The admittance derived from jreftran_rt.m, is consistent with the equation above (which relates the surface electric field to the admittance).

9.1.3 Sensitivity to contamination

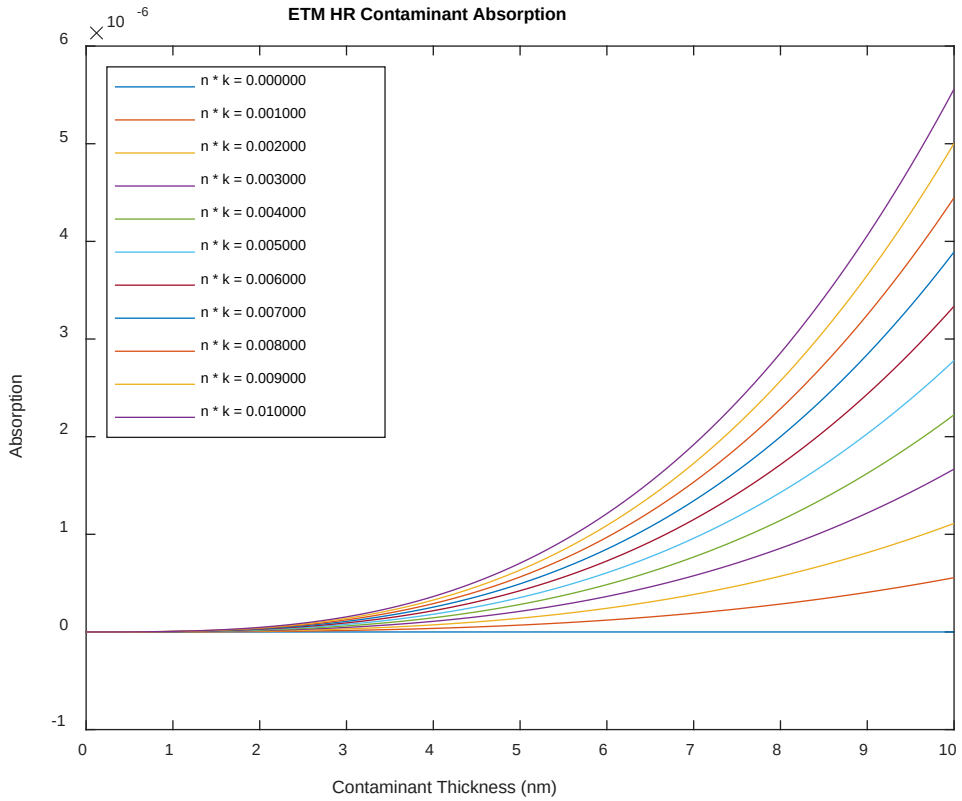

Figure 5 ETM HR coating absorption sensitivity to contamination layer

9.2 ETM AR

9.2.1 Specification

The Anti-Reflectance (AR) coating specification for the ETM is given in LIGO-E0900068 as follows:

- R < 500 ppm @1064 nm wavelength
- A < 1 ppm
- no requirement regarding the surface electric field

9.2.2 Coating design

LMA's proprietary ETM AR coating design is given in LIGO-C1000251. The reflectance and absorption calculated with a modified version of the Matlab script jreftrans_rt.m, agrees reasonably well with the specification:

- R = 26.0 ppm
- A = 1.4 ppm

The surface electric field value is E = 27.4 V/m.

9.2.3 Sensitivity to contamination

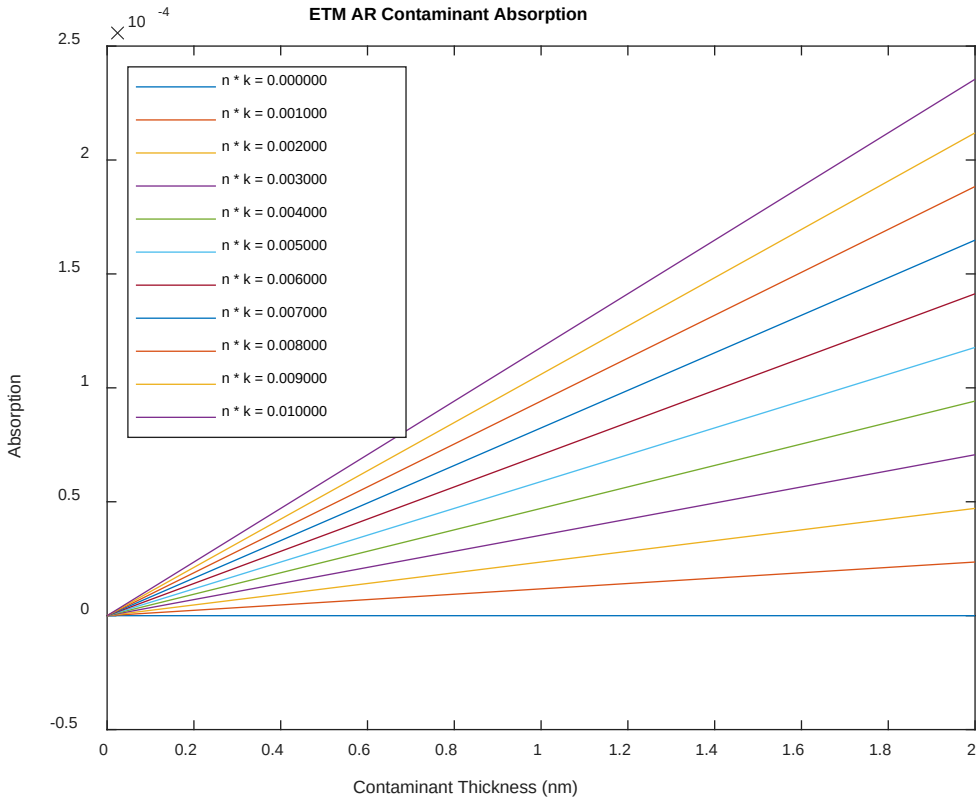

Figure 6 ETM AR coating absorption sensitivity to a contamination layer

9.3 ITM HR

9.3.1 Specification

The HR coating specification for the Input Test Mass (ITM) is given in https://dcc.ligo.org/LIGO-E0900041 as follows:

- T = 0.013 to 0.015 @ 1064 nm wavelength
- A < 0.5 ppm
- Surface electric field @1064 nm, E < 0.25 V/m

9.3.2 Coating design

LMA's proprietary ITM HR coating design is given in LIGO-C0901389. The transmission, absorption and electric field distribution for the ITM HR coating, calculated with a modified version of the Matlab script jreftrans_rt.m, agrees reasonably well with the specification:

- T = 0.0132
- A = 0.8 ppm
- E = 0.75 V/m

The admittance derived from jreftran_rt.m, is fairly consistent with the equation above (which relates the surface electric field to the admittance).

9.3.3 Sensitivity to contamination

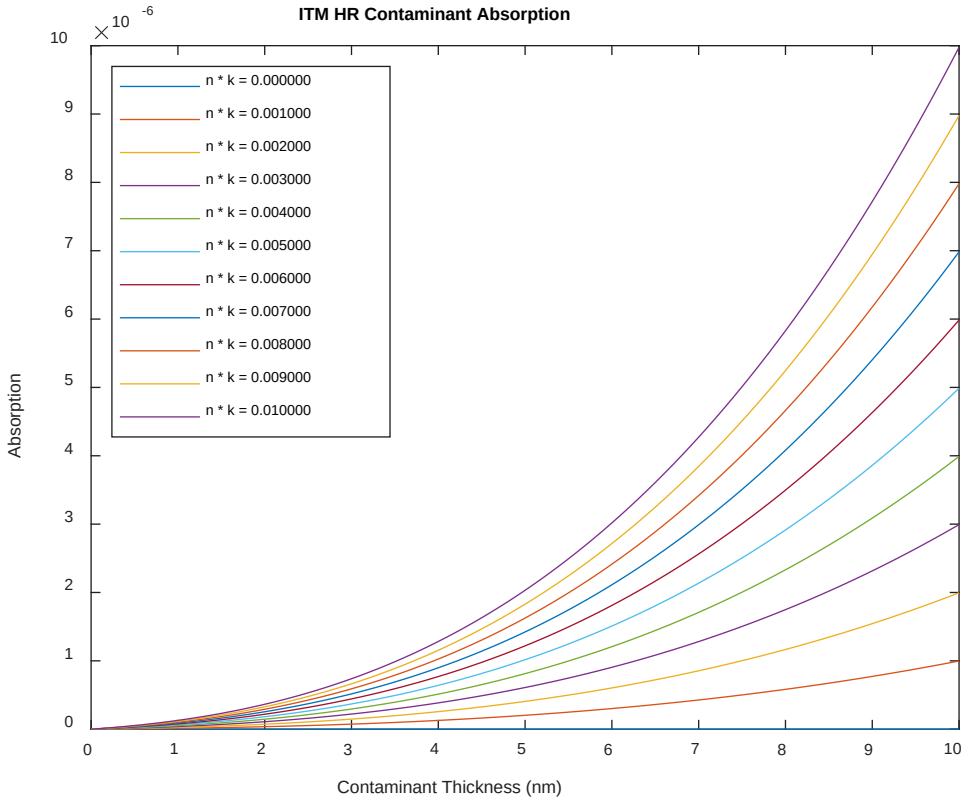

Figure 7 ITM HR coating absorption sensitivity to contamination layer

9.4 ITM AR

9.4.1 Specification

The Anti-Reflectance (AR) coating specification for the ETM is given in LIGO-E0900041 as follows:

- R < 50 ppm (goal < 20 ppm) @1064 nm wavelength
- A < 1 ppm
- no requirement regarding the surface electric field

9.4.2 Coating design

LMA's proprietary ETM AR coating design is given in LIGO-C1000140. The reflectance and absorption calculated with a modified version of the Matlab script jreftrans_rt.m, agrees reasonably well with the specification:

- R = 7.7 ppm
- A = 1.4 ppm

The surface electric field value is E = 27 V/m.

9.4.3 Sensitivity to contamination

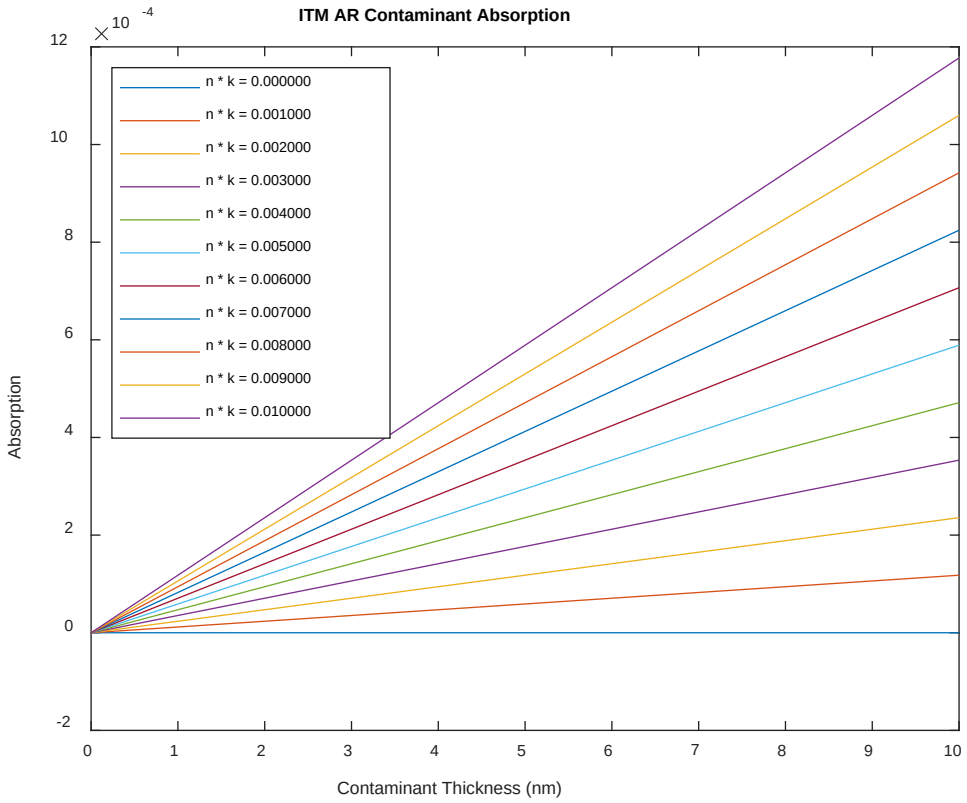

Figure 8 ITM AR coating absorption sensitivity to a contamination layer

9.5 Other LIGO optics

The LIGO core optics are listed at https://galaxy.ligo.caltech.edu/optics/. We generally do not have the details of the coating designs for the other LIGO optics. Consequently I'll assume that the contamination sensitivity of the test mass HR and AR coatings are representative of the other LIGO optics as well.

9.6 Allowable contamination deposition thickness

Given the sensitivity calculations in the above subsections, the absorption limits in section 2.4 and the three representative maximum n*k sets discussed in section 8, we can establish the hydrocarbon adsorption thicknesses limits shown in Table 4. If the maximum n * k values are in accordance with Set C (from Reference 33) then (as will be shown in section 10) there is absolutely no concern with molecular adsorption causing unacceptable optical absorption. However if the maximum n * k values are as indicated for Set B, then the AR absorption limits potentially set stringent requirements on the HC partial pressure. Set A is considered unrealistically pessimistic since it includes materials which are explicitly excluded from the vacuum system (grease, silicone and oil).

Table 4 Hydrocarbon adsorption thickness limits (nm)

		Maximum n * k		
Optic - coating	Absorption limit	Set A: .064 pessimistic	Set B: .0035 conservative	Set C: 3 x 10^{-6} possible
ETM - HR	< 0.5 ppm	2.4	6.3	68
ITM - HR	< 0.5 ppm	0.7	4.2	66
ETM - AR	< 4 ppm	.005	.097	113
ITM - AR	< 4 ppm	.005	.097	113

10 Hydrocarbon molecular adsorption

10.1 Adsorption density dependence on molecular weight

The binding energy of an adsorbed molecule increases as the molecular size (weight) increases. However, the outgassing rate (and vapor pressure) decrease with molecular weight. One then expects that the overall adsorption model[43] to behave as indicated in Figure 9.

Figure 9 Steady-state Adsorption Model[44] (independent of photodissociation and direct molecular streaming)

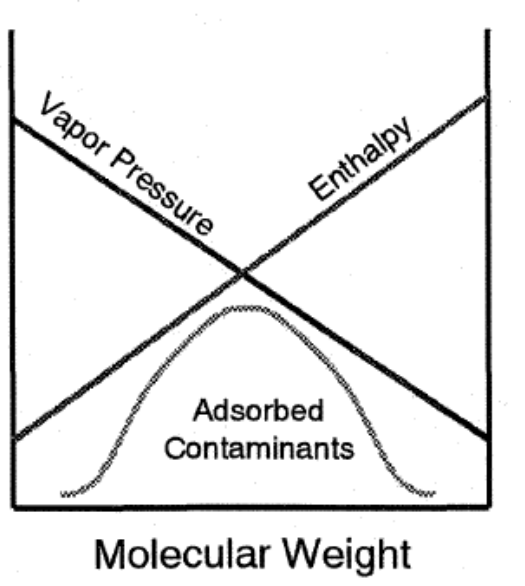

(a) Figure 8 from Reference [42]; at atmospheric conditions

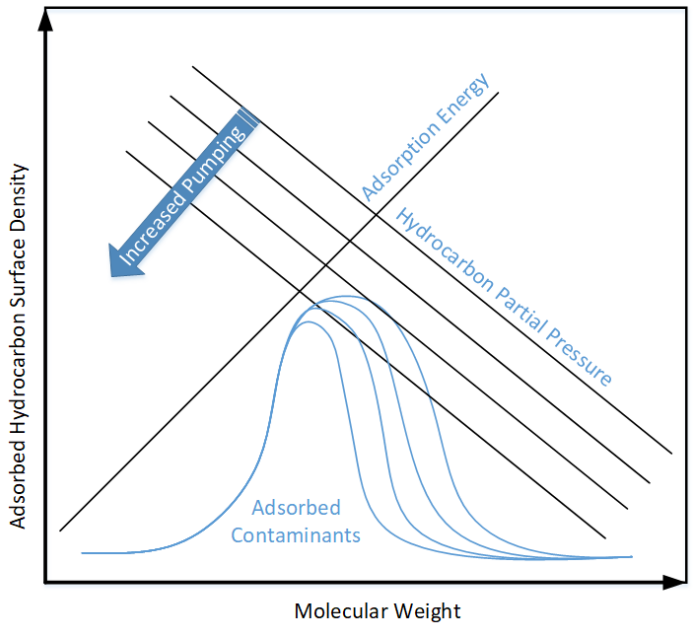

(b) Generalized to vacuum conditions

The adsorption density as a function of molecular weight was experimentally determined for silicon surfaces[43], at atmospheric pressure, to be as shown in Figure 10. If this result for Si at atmospheric pressure applies equally to our SiO2 optics at high vacuum conditions, then we may "only" need to address hydrocarbons with molecular weight < ~400 AMU.

Figure 10 Adsorbed density of aliphatic hydrocarbons on Si as a function of molecular weight at atmospheric pressure

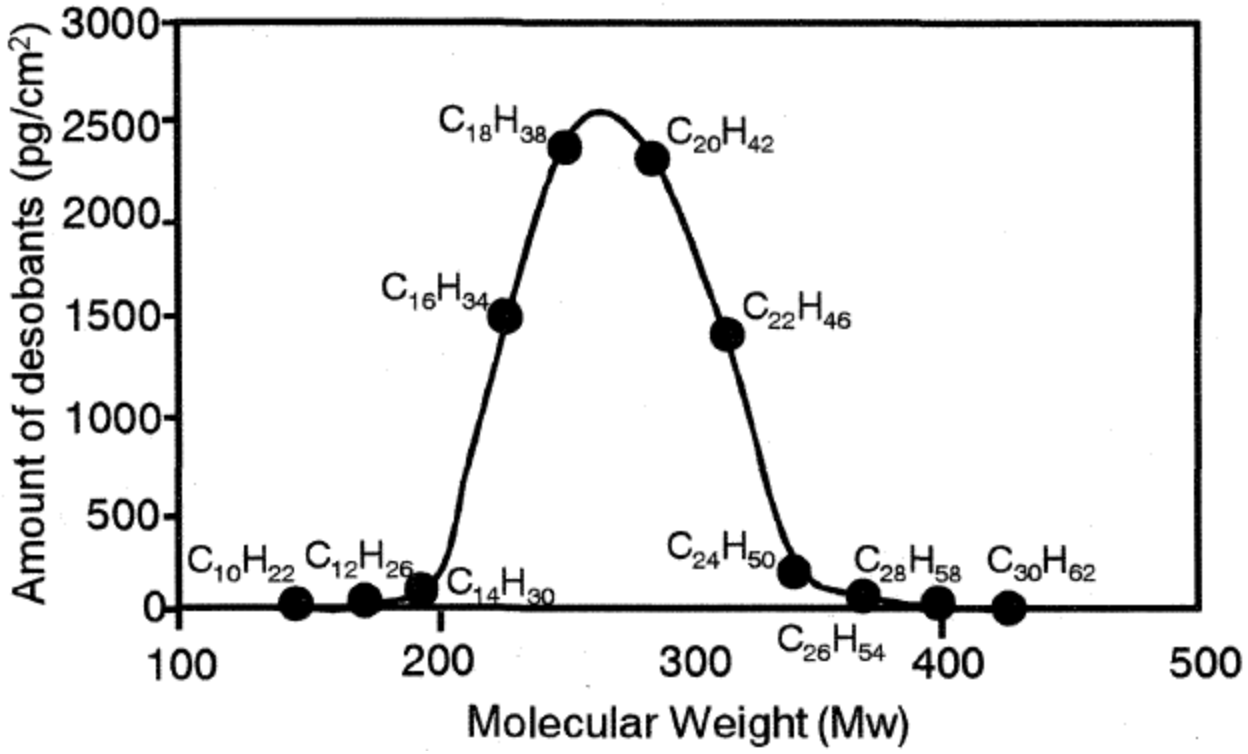

10.2 Vapor pressure and outgassing rate vs molar mass

Ideally we would like a sensitive RGA scan (accumulation scan) of the LIGO Observatory vacuum volumes up to ~500 AMU. This data could then be used to estimate the adsorbed species composition and surface density and ultimate yield an estimate of the optical degradation effects.

In addition to the high AMU RGA, crystal quartz microbalances should be used to determine the adsorption rate. Ideally these measurements would be made as a function of temperature and the adsorbed species extracted and analyzed for composition.

Without a high AMU RGA scan we can only attempt a rough estimate of the partial pressure of high AMU components. The vapor (saturation) pressure for hydrocarbons (polymers) generally decreases as the molar mass increases, as indicated in Figure 11. Likewise the hydrocarbon outgassing rates will generally decrease as the molar mass increases. Without a high AMU RGA scan, it would be useful to develop a general correlation, or bound, on the hydrocarbon areal outgassing rates (Torr-L/s/cm^2) as a function of molecular weight of the outgassed species, for all hydrocarbon materials which might be permitted in our vacuum system. With such data we could estimate the partial pressure as a function of AMU given our pumping speeds. The RGA scans from our vacuum bake

loads of parts are not adequate for this purpose; These scans are typically only bounds. I think that the data exists in the literature although there may be considerable uncertainty and scatter in the data.

Figure 11 Vapor pressure vs molar mass for a selection of hydrocarbons

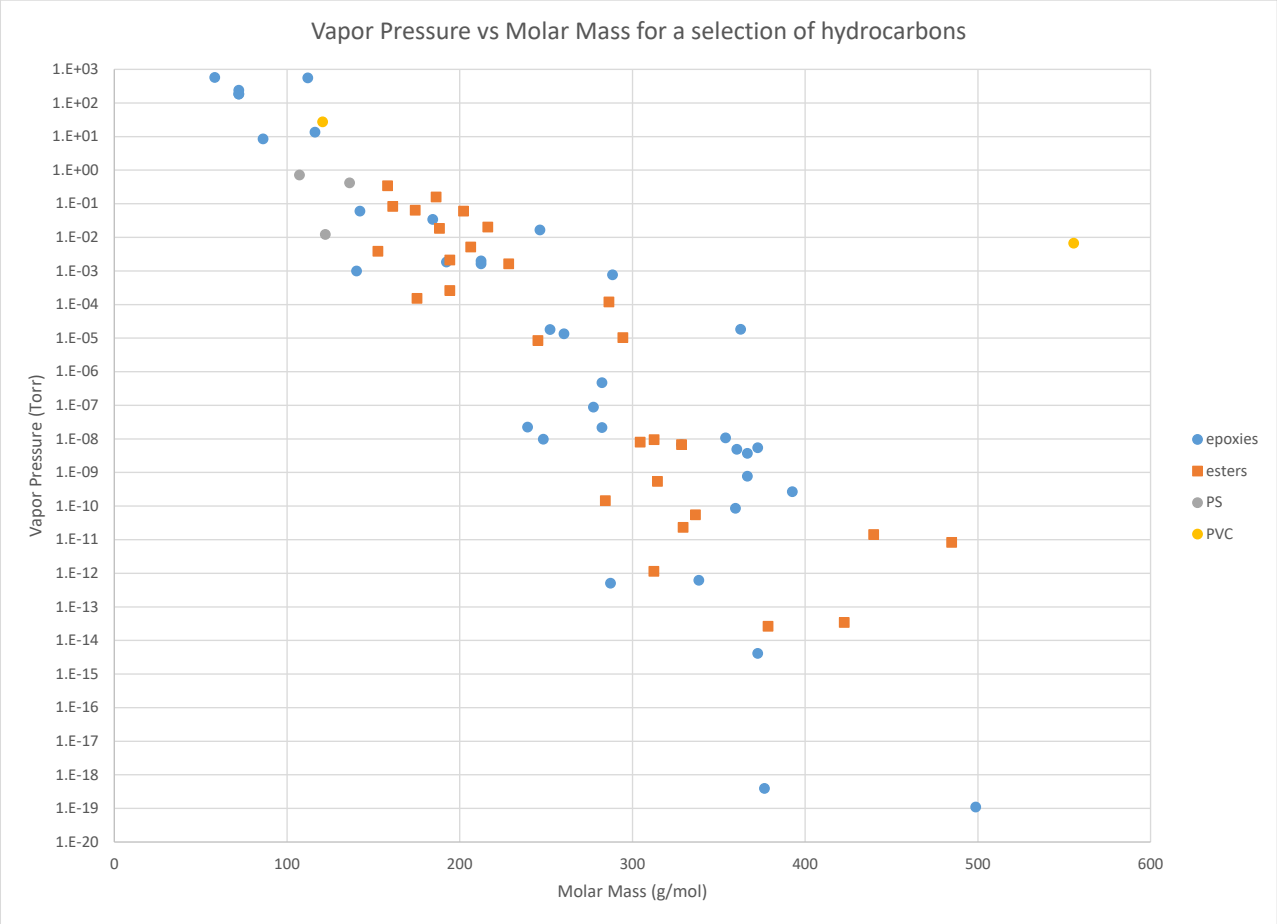

10.3 Monolayer thickness vs molar mass

Using molar mass and density the diameter of an equivalent spherical molecule can be calculated as an approximation of the monolayer thickness, as shown in Figure 12. The monolayer thicknesses of 5 fatty acids (with molar masses about ~300 g/mol) measured via Brewster angle microscopy[45] compare reasonably well (-13%/+27%) to these approximate spherical diameters.

Figure 12 Approximate monolayer thickness vs molar mass for a selection of hydrocarbons

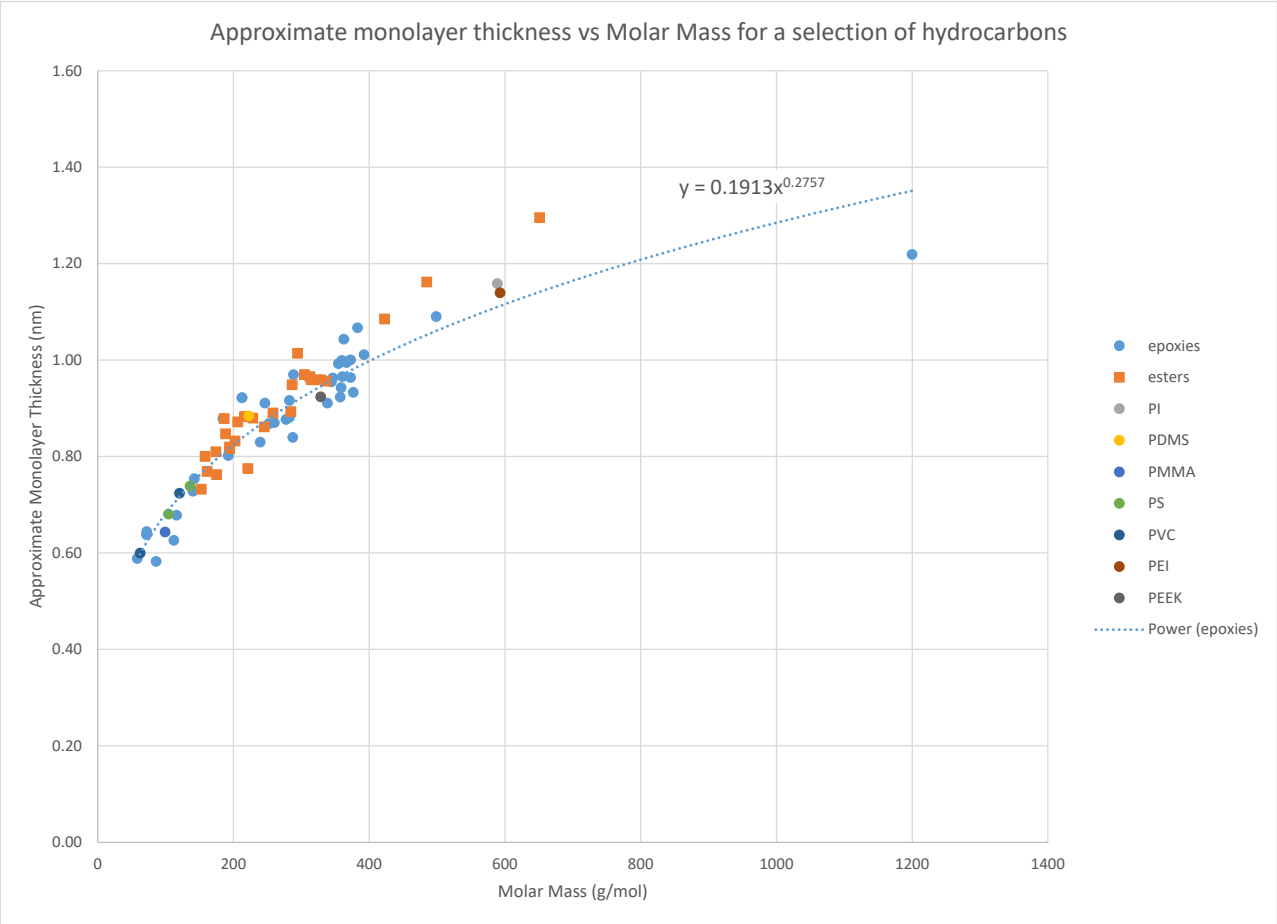

10.4 Adsorption isotherms

The steady-state adsorbed molecular density on a surface is the result of equilibrium between the molecular impingement rate from the gas above the surface and the thermal desorption from the surface (which depends on the binding energy which may be temperature dependent). Commonly used models[46] to describe the equilibrium dynamics and the resulting surface coverage are the Langmuir, Temkin, Freundlich and Dubinin-Radushkevich isotherm models. The Langmuir isotherm[47] assumes a constant adsorption energy (for each molecular species), and results in surface coverage that is approximately linear in pressure over limited pressure ranges. The Temkin isotherm[48] includes a term that is proportional to the surface coverage to account for site competition, which results in a surface coverage that depends on the logarithm of the pressure over limited ranges. Two experimental studies[46,23] on EUV induced carbon growth at low vacuum pressures indicated that these isotherms/models under-predict the carbon growth at low pressures, which prompted development/application of revised coverage-dependent adsorption energy models/isotherms. The Hollenshead 2019 study [23] used the Nitta Multisite Absorption (NMA) isotherm which accounts for entropy (configuration) effects on the binding of large molecules to surfaces. Large linear molecules bind to surfaces with their carbon chains parallel to the surface, requiring higher adsorption energy and multiple, contiguous surface sites. Nitta et. al. have shown that large hydrocarbon molecules follow the NMA isotherm:

$$n\,K\,P = \frac{\theta}{(1-\theta)^n}$$

where

n = number of contiguous surface sites

θ = fractional surface coverage

K = equilibrium constant for adsorption

P = partial pressure

The NMA isotherm reduces to the Langmuir isotherm when n = 1.

The weak interaction between gas-phase hydrocarbons and adsorbed hydrocarbons, there is little tendency to grow more than one monolayer (until the saturation pressure is exceeded), so

$$\theta = \frac{N_{ad}}{N_{ad}^{max}}\ where\ N_{ad}^{max} = 1\ monolayer$$

In steady-state, the adsorbed number density, N_{ad}, is given by a balance between the impingement flux, s Γ_{mol}, and the thermal desorption rate:

$$N_{ad}^{ss} = \frac{s\,\Gamma_{mol}}{v_0 e^{\left(-E_a/R\,T\right)} + \frac{s\,\Gamma_{mol}}{N_{ad}^{max}}}$$

where

v0 ≡ 10^{13} 1/s, ~the vibration frequency of the adsorbed molecules

E_a = molecular adsorption energy, kJ/mol

R = universal gas constant

T = temperature of the optic surface

s ≡ 1, the condensation coefficient, i.e. all molecules impinging on the surface are adsorbed if only for a short time. This is not the same as a sticking coefficient.

Γ_{mol} = the impingement rate from the kinetic theory of gases (which depends on the temperature and the partial pressure)

An infrared characterization[49] of some optical substrate materials with and without coatings (CaF2, Si and ThF4 coated CaF2), using multiple internal-reflection (MIR) spectroscopy indicates hydrocarbon film saturation from laboratory air exposure (and in proximity or contact with a Delrin holder) at 1.8 nm after 200 hr. A similar study[50] using MIR spectroscopy measured a 1.3 nm HC film on Si. The rate of HC contamination is not repeatable, since it will depend upon the level of HC vapor in the atmosphere, but the saturation level should be repeatable. These results suggest that typical hydrocarbon surface areal saturation may occur for just 1 or 2 monolayers.

More relevant to LIGO are a number of studies that indicate that a single monolayer adsorption of hydrocarbon films occurs only at partial pressures approaching the saturation (vapor) pressure of the molecular species.

10.5 HC adsorption on Ru

One model, which successfully predicts radiation-induced carbon contamination of EUV optics, has been used to calculate the steady-state adsorbed surface density for the following four hydrocarbons on Ru surfaces, as shown in Figure 13:

- n-tetradecane (C14H30), 198.39 g/mol, 0.767 g/cc, Ea = 96.35 kJ/mol
- n-dodecane (C12H26), 170.34 g/mol, 0.753 g/cc, Ea = 85.13 kJ/mol
- n-decane (C10H22), 142.282 g/mol, 0.734 g/cc, Ea = 73.90 kJ/mol, 1.58 Torr vapor pressure
- benzene (C6H6), 78.11 g/mol, 0.879 g/cc, Ea = 85.07 kJ/mol, 100 Torr vapor pressure

At a partial pressure of ~1 pTorr the steady-state adsorbed surface density is < 1% of a monolayer.

Figure 13 Steady-state surface density of four hydrocarbons on Ru surface, in the partial pressure range from 1 pTorr to 0.1 Torr

Calculation based on the model in Reference 23: Steady-state surface density as a function of pressure for n-tetradecane, n-dodecane, n-decane, and benzene from 10^{-12} to 0.1 Torr without photodissociation. The optic temperature is 298.15 K. Solid lines are NMA isotherms. Dashed lines are Langmuir isotherms. The dotted line is transcribed from Figure 6 of Reference 46 for n-tetradecane using an alternative adsorption isotherm. (a) Full range and (b) expanded abscissa and ordinate scales.

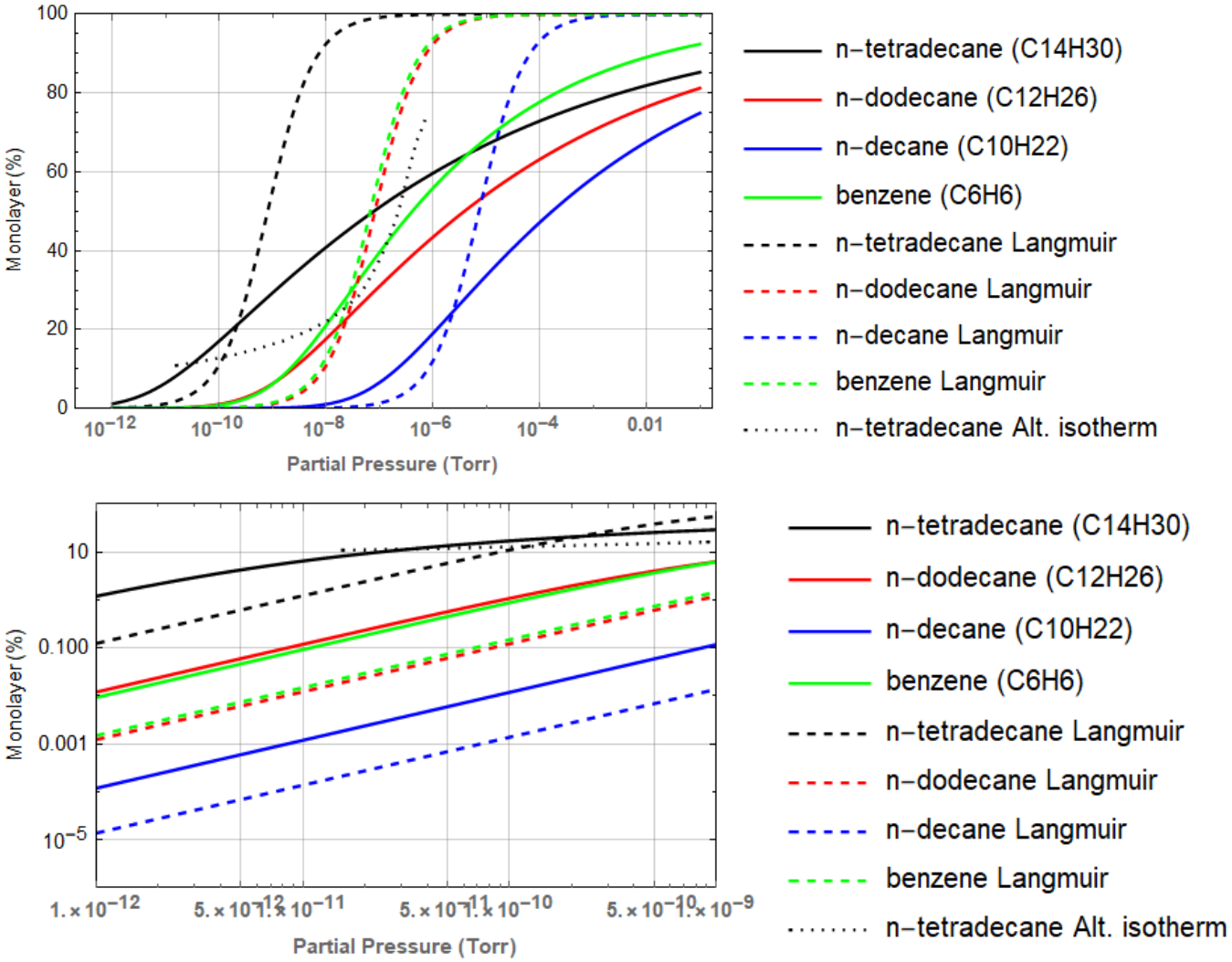

If these four HC contaminants were the only ones that we needed to worry about, and if our optics were capped with Ru, then we could conclude that our HC partial pressure limit is < 10^{-11} Torr. However, we need to consider other HCs, potentially with AMUs up to ~400, and we need to consider adsorption on SiO2.

10.6 HC adsorption as a function of molar mass

In a key paper regarding modeling of radiation-induced carbon contamination of EUV optics (Reference [23]), the authors stated that they linearly extrapolated the n parameter fits to the NMA isotherms for their hydrocarbons based on "chain length". In the paper in which the NMA isotherm was proposed (T. Nitta, T. Shigetomi, M, Huro-oka and T. Katayame, 1984), the authors plotted n versus the "molecular area projected on a plane", which is also labeled "molecular cross-sectional area". They calculated the molecular areas by means of compiled values of the van der Waals radii and bond lengths. The NMA n-parameter vs molecular area fit and the apparent molecular areas for the HCs used in Reference [23] are shown in Figure 14.

Figure 14 Linear fit of the NMA isotherm parameter "n" with molecular cross-sectional area

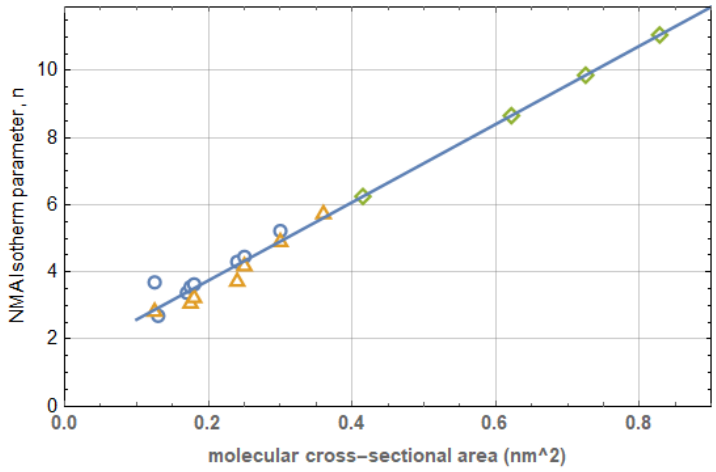

I searched the literature for molecular size, area, cross-sectional area, van der Waals volume, bond length, etc. to no avail. However, the NMS n-parameter appears to be linearly related to the molecular weight as indicated in Figure 15.

Figure 15 Linear fit of the NMA isotherm parameter "n" with molecular weight

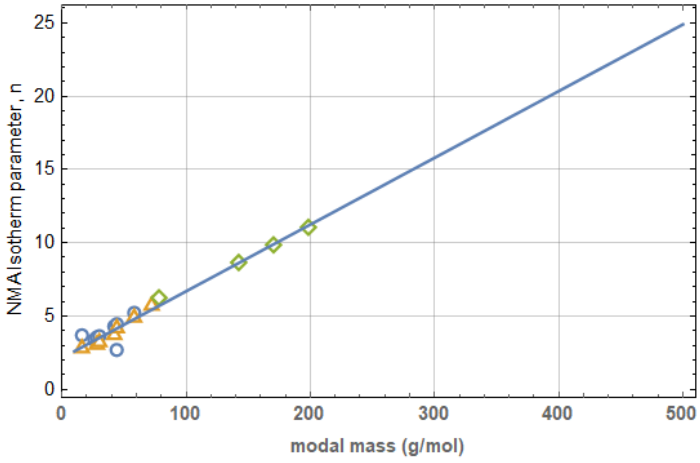

The authors of Reference [23] note (in the supplemental material) that the spread of HC binding energies, observed on various substrates for coverages up to 1 monolayer, is only ± 1.5 kJ/mol, i.e. negligible. If we accept this argument then we can use the same binding energy (adsorption energy) used in this reference for adsorption to our SiO2 optics. Nonetheless, it would be good to get definitive, trusted sources for HC adsorption energies for SiO2 surfaces as a check if nothing else.

As for other HCs, up to AMU 400, it would be good to be able to consider all possible HCs and set partial pressure limits to ensure that our optics do not degrade more than allowable. If this is not possible, then the alternative is to set limits on HC contaminants either known or suspected of being present in our vacuum system.

The desorption energies, E_{ad}, for straight chain alkanes ($H(CH_2)_nH$ with n = 5 to 60) has been found[51] to fit the equation $E_{ad} = -29 + 42\ n^{0.5}$ with $5 \le n \le 60$, spanning molar mass from 72 to 844 g/mol. In another study[52] the desorption energy for small alkanes (1<n<10) was found to vary significantly with coverage; The desorption energy decreases rapidly from 0 to ~0.1 monolayers and then varies linearly (and slightly). The value of the adsorption energy in this linear region, projected back to the limit of zero coverage is E0 = 5.4+7.2 n with $1 \le n \le 5$. The desorption energy for these straight chain alkanes are plotted with other HC adsorption energies from the literature in Figure 16. Note that there appears to be a lot of scatter in the data (other than for straight chain alkanes from Reference [51]). The values of the adsorption energies for the three alkanes used in Reference [23] (i.e. n-tetradecane, n-dodecane and n-decane) are considerably less than those from Reference [51], despite the fact that n-dodecane and n-decane are straight chain alkanes. (N-tetradecane has a slightly different structure at the termini of the chain, $CH_3(CH_2)_{12}CH_3$.) However the Reference [23] values are consistent with Reference [52] values. Since the adsorption energy has a very significant impact on the steady-state coverage values (monolayers), this discrepancy is significant. For the adsorption model presented below, I choose to uniformly shift the adsorption energy values/equation from Reference [51] to match the values from Reference [52] as an expedient means of approximating the adsorption energy values > ~0.1 ML and capturing the square root dependence on alkane chain length.

Figure 16 HC adsorption energy vs molar mass

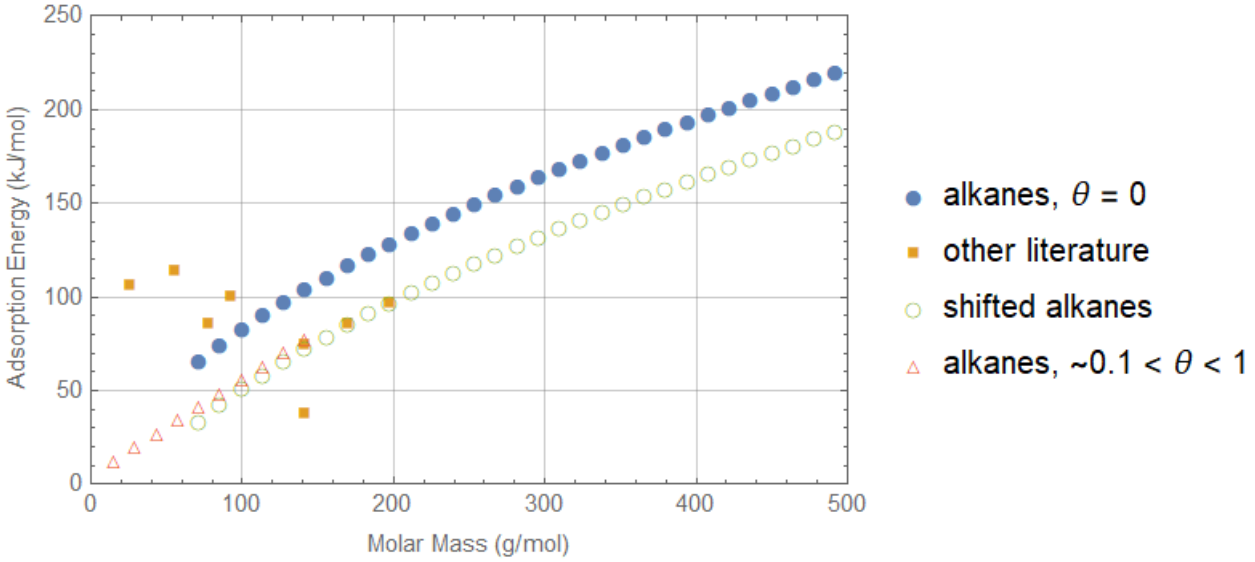

Using the correlations of adsorption energy and the n-parameter of the NMA isotherm with molecular weight, we can project the expected adsorption coverage as a function of molecular weight, as shown

in Figure 17. If the "conservative" (Set B) values of the refractive indices of the hydrocarbon contaminants are correct (see section 9.6), then we should limit adsorption thickness to 0.1 nm, or ~0.13 monolayer (since a 200 AMU ML = 0.8 nm). For our estimate of hydrocarbon partial pressure, 3 pTorr (see section 2.1.1), this corresponds to ~200 AMU. Note that the required partial pressure for higher AMUs increases quite quickly; From Figure 17, the partial pressure for AMU 226 should be < 10^{-16} Torr to ensure an adsorbed thickness of < 0.13 ML.

Figure 17 Hydrocarbon steady-state adsorption as a function of molecular weight

Calculation based on the model in Reference 23, without photodissociation. (a) Full range and (b) expanded abscissa and ordinate scales. Values called out on the right side for each curve are the molecular weights (g/mol).

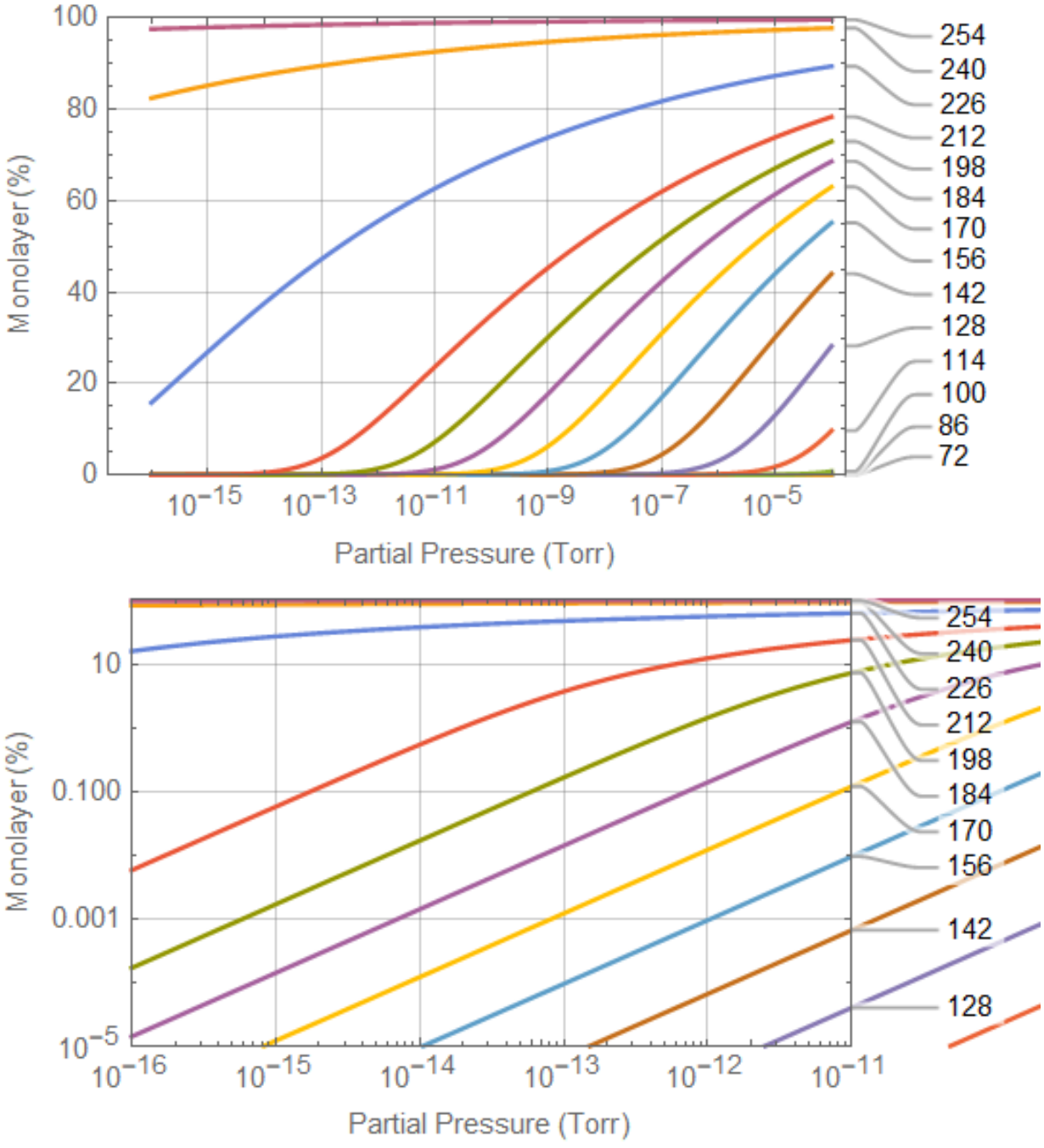

11 Recommendations

Not all of the following recommendations are of equal importance. I leave it to the Vacuum Review Board (VRB) to decide priorities:

1) Better limits on the corner and end station HC PP based on scattered light phase noise considerations: Although the hydrocarbon partial pressures limits derived in Reference [1] and listed in section 1 of this memo still apply, the allowable partial pressures in the vertex and end stations can be higher due to the attenuation through the cryopumps and the fact that the beam tube surface acts as a near infinite capacity pump. Calculate a proper limit of the corner and end station HC PPs.
2) Our optical ring-down cavities used for material qualification are insensitive to the effects of adsorbed contamination by the nature of the HR coatings used in these optical cavities. While this is a faithful emulation of our HR coated core optics, it would be better to employ HR coatings which are intentionally designed to be more sensitive to the adsorbed contaminant so that we can measure the effect and use modeling to scale to the LIGO observatory conditions. In addition, our optical ring-down cavities have fluence levels which are somewhat less than the peak fluence levels planned for aLIGO/A+. The finesse of the cavities should be increased to achieve the same peak fluence levels that we plan to ultimately achieve in aLIGO/A+.
3) Confirm that Multiple Photon Dissociation (MPD) is not a risk for LIGO at the ultimate aLIGO/A+ fluence levels by applying the model developed in Reference [23].
4) Conduct a literature review (and experimentation if necessary) to establish a scattering loss model from fused silica, as a function of HC adsorbed sub-monolayer thickness for representative HCs.
5) Our current RGA units only measure to AMU 100. RGA units capable of measuring up to AMU 500 should be used to make sensitive measurements (accumulation scans) of the partial pressures of high AMU components in the Observatory vacuum system.
6) Crystal quartz microbalances should be used to determine the adsorption rate. Ideally these measurements would be made as a function of temperature and the adsorbed species extracted and analyzed for composition.
7) Develop a general correlation, or bound, on the hydrocarbon areal outgassing rates (Torr-L/s/cm2) as a function of molecular weight of the outgassed species, for all hydrocarbon materials which might be permitted in our vacuum system. I think that the data exists in the literature although there may be considerable uncertainty and scatter in the data.
8) Resolve the apparent discrepancy in the literature regarding the extinction coefficients for outgassed HC species. This might be done by first careful peer review of the methodology employed by various studies. If the claim by the authors of Reference [33] that their technique is more accurate for measurement of the low extinction coefficients typical for the outgassed HCs, then consider employing this team to make further measurements relevant to LIGO, or replicating their measurement system for our use.

12 Summary

A framework for determining the required limits on hydrocarbon partial pressure as a function of molecular weight has been presented. The determination of the sensitivity of the optical coatings

requires knowledge of the details of the multi-layer dielectric coatings as well as the complex refraction properties of potential hydrocarbon contaminant films. We can adopt and adapt the adsorption and photodissociation modeling work from the EUV community to further modeling and understanding for LIGO. In particular a general formulation using correlations to molecular weight can be used to bound the requirements for LIGO. It is my hope that a better understanding of the HC partial pressure requirements might lead to (a) a reduction in the enormous amount of work spent qualifying materials and (b) allowing more materials to be used in the design of the LIGO interferometer components.

A conservative estimate of the maximum allowed hydrocarbon partial pressure based on the molecular impingement flux and an assumption of unity sticking coefficient results in a partial pressure requirement of < 5 x 10-15 Torr. Our aLIGO vacuum performace is ~3 x 10-12 Torr, a factor of ~1000 higher. Yet we have not observed any significant optical absorption increase to date. The analysis presented in the memo suggests several possible contributing explanations:

a) The components of our hydrocarbon partial pressure (measured as cracked fragments at AMUs 41, 43, 53, 55 and 57) may be dominated by low AMU hydrocarbons. These low AMU HCs have short adsorption residence times and so do not contribute to a steady-state, significant thickness of an adsorption layer.
b) The HR coatings are inherently weakly sensitive to adsorbed contaminants since their surface electric field is designed to be near zero. (Conversely the AR coatings are rather sensitive to the adsorbed contaminant layer, although we can tolerate somewhat more absorption on the AR coatings.)
c) The extinction coefficients of the outgassed and adsorbed HCs may be extremely small, as suggested by the measurements in Reference [33].
d) The adsorption thickness at LIGO HV/UHV partial pressures self-limit to < 1 monolayer.

The LIGO hydrocarbon partial pressures have been shown to be ~ 5 times less than found in a EUVL test system at Sandia National Labs. Given the significant concerns regarding carbon growth on EUV optics due to photodissociation of adsorbed hydrocarbon contaminants, considerable care is taken in the selection of materials and their preparation for EUV system. From this comparison we can infer that the LIGO vacuum system protocols for material selection and preparation (cleaning, baking) are reasonable. (Of course since the LIGO and EUVL applications are quite different we cannot draw any further inferences.)

A number of other recommendations have also been proposed. The two most significant recommendation are to redesign the material qualification ring-down cavities to be more sensitive to the adsorbed contaminant and to get a better understanding of the extinction coefficients of the outgassed and adsorbed contaminants.

---

[1] Vacuum Hydrocarbon Outgassing Requirements, LIGO-T040001
[2] Beam Tube Modules, LIGO-G950082
[3] Section 4 of "aLIGO System Acceptance Document/Data Package", LIGO-E1400371
[4] This requirement is articulated in LIGO-E1000731, but the original source has not been found.
[5] See for example data from the Beam Tube bake and pump-down: https://dcc.ligo.org/LIGO-T960124, https://dcc.ligo.org/LIGO-T970110 and https://dcc.ligo.org/LIGO-T970111
[6] "RGA Test Qualification of components for the LIGO UHV", https://dcc.ligo.org/LIGO-E080177
[7] Section 5 of LIGO-L2100162
[8] LLO elog #58480

[9] Section 3 of LIGO-T000055
[10] "LIGO Vacuum Compatible Materials Qualification", https://dcc.ligo.org/LIGO-G2101787
[11] "Qualifying Parts for LIGO UHV Service", https://dcc.ligo.org/LIGO-E1000088
[12] "Optical Contamination Screening of Materials with a High-finesse Fabry-Perot Cavity Resonated Continuously at 1.06-um Wavelength in Vacuum", https://dcc.ligo.org/LIGO-P990032
[13] LIGO UHV Qualification Test Results, LIGO-E1000193
[14] J. Camp, "Surface Analysis of Damaged Resonator Mirrors", LIGO-T2200037, 1993.
[15] J. Hollenshead and L. Klebanoff, "Modeling radiation-induced carbon contamination of extreme ultraviolet optics", J. Vac. Sci. Technol. B 24(1), Jan/Feb 2006.
[16] Osantowski, J., "Contamination sensitivity of typical mirror coatings – a parametric study", Proc. SPIE 0338, Spacecraft Contamination Environment, 12 Apr 1983; doi: 10.1117/12.933641
[17] Hass, G. and Hunter, W.R., "Laboratory experiments to study surface contamination and degradation of optical coatings and materials in simulated space environments", Applied Optics, v9, n4, 2101 (1970).
[18] Hunter, W.R., "Optical Contamination: its prevention in the XUV spectrographs flown by the U.S. Naval Research Laboratory in the Apollo Telescope Mount", Applied Optics, v16, n4, Apr 1977.
[19] Ternet, Barrie, Olson, "Optical scatter from nonuniform molecular films", Proc. SPIE 5526, Optical Systems Degradation, Contamination and Stray Light: Effects, Measurements, and Control, 15 Oct 2004. Doi: 10.1117/12.556121
[20] K. Boller, R.P. Haelbich, H. Hogrefe, W. Jark and C. Kunz, "Investigation of carbon contamination of mirror surfaces exposed to synchrotron radiation", Nuclear Instruments and Methods, 208 (1983), pp 273-279.
[21] R. Kurt, M. van Beek, C. Crombeen, P. Zalm, Y. Tamminga, "Radiation induced carbon contamination of optics", Proc. SPIE, v 4688 (2002)
[22] J. Hollenshead, L. Klebanoff, "Modeling radiation-induced carbon contamination of extreme ultraviolet optics", J. Vac. Sci. Technol. B 24(1), Jan/Feb 2006.
[23] J. Hollenshead, L. Klebanoff and G. Delgado, "Predicting radiation-induced carbon contamination of EUV optics", J. Vac. Sci. Technol. B 37, 021602 (219).
[24] S.B. Hill, C. Tarrio, R.F. Berg, T.B. Lucatorto, "Extreme-ultraviolet-induced carbon growth at contaminant pressures between 10-10 and 10-6 mbar: Experiment and model", J. Vac. Sci. Technol. A 38(6), Nov/Dec 2020.
[25] Welsh, Barry and Jelinsky, Sharon, "The effect of out-gassing from commonly used spacecraft/space instrument materials on the UV-visible-IR reflectivity of optical surfaces", Proc. SPIE 5897, Photonics for Space Environments X, 58970B (30 Aug 2005); doi: 10.1117/12.614178
[26] The article mentions use of a MaxTek™ (now Inficon) quartz crystal microbalance. An online operating manual (https://www.inficon.com/en/products/discontinued-maxtek) implies that the surface is gold plated.
[27] Shimazaki, Kazunori ; Miyazaki, Eiji ; Kimoto, Yugo, "Optical changes of molecular contamination thin-film outgassed from epoxy-based resin during deposition and desorption process", Acta Astronautica, DOI: 10.1016 / j.actaastro.2018.07.010, July, 2018
[28] Both studies employed vacuum systems with turbomolecular pumps. The Welsh and Jelinsky study noted pressures < 10^{-4} Torr with a bell jar system sealed with an elastomeric gasket. The Shimazaki et. al. study did not note the vacuum pressure but used a cryogenic shroud cooled by liquid nitrogen within a stainless steel vessel presumable sealed with copper gaskets.
[29] section 2.1.3.2 of A.C. Tribble, Fundamentals of Contamination Control, SPIE Vol TT44, 2000, ISBN: 9780819438447
[30] section 2.1.3.2 of A.C. Tribble, et. al., "Contamination Control Engineering Design Guidelines for the Aerospace Community", NASA Contractor Report 4740, May 1996.
[31] Equation 2.135 of H.A. Macleod, Thin-Film Optical Filters, 3rd ed., cr 2001, Institute of Physics Publishing, ISBN 0 7503 0688 2. See also section 10.2, "sensitivity to contamination".
[32] Xiaoning Zhang, Jun Qiu, Junming Zhao, Xingcan Li, Linhua Liu,"Complex refractive indices measurements of polymers in infrared bands", Journal of Quantitative Spectroscopy & Radiative Transfer 252 (2020) 107063
[33] Xiaoning Zhang, Jun Qiu, Xingcan Li, Junming Zhao, and Linhua Liu, "Complex refractive indices measurements of polymers in visible and near-infrared bands", Applied Optics, Vol. 59, No. 8 , 10 March 2020, pg 2337
[34] C Hughes, G Workman, J Reynolds, "Use of variable angle spectroscopic ellipsometry in order to determine contaminant optical properties", 2nd Aerospace Environmental Technology Conference, 1997 , pp.329-334
[35] P. Boeder, et.al., "Effect of a silicone contaminant film on the transmittance properties of AR-coated fused silica", Proc. SPIE 5526, Optical Systems Degradation, Contamination and Stray Light: Effects, Measurements and Control, 15 Oct 2004; doi: 10.1117/12.560859

[36] H.S. Judeikis, G.S. Arnold, M. Hill, R.C. Young Owl and D.F. Hall, "Design of a Laboratory Study of Contaminant Film Darkening in Space," Scatter from Optical Components, Proceedings from the International Society for Optical Engineering, Vol. 1165, San Diego, California, August 1989, pp 406-423.
[37] B.E. Wood, P.M. Falco and J.D. Holt, "Satellite material contaminant optical properties", N90-25529, 3rd annual workshop on Space Operations Automation and Robotics, SOAR 1989, p 257-262.
[38] C.C. Wang, J.Y. Tan, Y.Q. Ma and L.H. Lui, "Infrared optical constants of liquid palm oil and palm oil biodiesel determined by the combined ellipsometry-transmission method", Applied Optics, v 56, n 18, Jun 2017, https://doi.org/10.1364/AO.56.005156
[39] J. Bauer, et. al., "Novel UV-transparent 2-component polyurethane resin for chip-on-board LED micro lenses", Vol. 10, No. 9 / 1 September 2020 / Optical Materials Express
[40] M.A. El-Rahman, et. al., "Effect of gamma radiation on the optical properties of epoxy resin thin films", Optik, v 183 (2019), 962-970.
[41] equation 2.132 from H.A. Macleod, Thin-Film Optical Filters, 3rd ed., cr 2001, Institute of Physics Publishing, ISBN 0 7503 0688 2.
[42] jreftran_rt.m was written by Dawn Divitt (ETH Zurich Photonics group) and is available at this link: https://www.mathworks.com/matlabcentral/fileexchange/50923-jreftran-a-layered-thin-film-transmission-and-reflection-coefficient-calculator?s_tid=srchtitle_jreftrans_1
jreftran_rt.m is based on the formulation and matlab script jreftran.m documented in Kenneth Pascoe, "Reflectivity and Transmissivity through Layered, Lossy Media: A User-Friendly Approach", AFIT/EN-TR-01-07 Technical Report, Feb 2001.
My modification to jreftran_rt.m was to calculate the electric field distribution through the coating.
[43] M. Nagase, M. Kitano, Y. Wakayama, Y. Shirai and T. Ohmi, "Influence of molecular weight of organic contaminants upon adsorption behaviors onto silicon surfaces", Electrochemical Society Proceedings, v 2001-26.
[44] Figure 8 from Reference 43
[45] Fidalgo Rodríguez, J., Dynarowicz-Latka, P., & Miñones Conde, J. (2017). Structure of unsaturated fatty acids in 2D system. Colloids and surfaces. B, Biointerfaces, 158, 634-642.
[46] S. Hill, C. Tarrio, R. Berg and T. Lucatorto, "Extreme-ultraviolet-induced carbon growth at contaminant pressures between 10-10 and 10-6 mbar: Experiment and model", J. Vac. SCI. technol., A 38(6), Nov/Dec 2020.
[47] I. Langmuir, J. Am. Chem. Sci. 40, 1361 (1918).
[48] M.I. Temkin and V. Pyzhov, Acta Physicochim. URSS 12, 217 (1940).
[49] E.D. Palik, J.W. Gibson, R.T. Holm, H. Hass, M. Braunstein and B. Garcia, "Infrared characterization of surfaces and coatings by internal-reflection spectroscopy", Applied Optics, v 17, n11, June 1978.
[50] J.E. Olsen and F. Shimura, "Infrared analysis of film growth on the silicon surface in room air", J. Vac. Sci. Technol., A 7 (6), Nov/Dec 1989.
[51] K.R. Paserba and A,J, Gellman, "Kinetics and energetics of oligomer desorption from surfaces", Physical Review Letters, v86 n19, May 2001.
[52] S. Tait, Z. Dohnalek, C. Campbell, B. Kay, "n-alkanes on MgO(100). II. Chain length dependence of kinetic desorption parameters for small alkanes", J. Chem. Phys. 122, 164708 (2005).